Position and Ionization State of Asp in the Core of Membrane-Inserted α Helices Control Both the Equilibrium between Transmembrane and Nontransmembrane Helix Topography and Transmembrane Helix Positioning†

Gregory A. Caputo‡,|| and Erwin London*,‡,§

Department of Biochemistry and Cell Biology and Department of Chemistry, Stony Brook University, State University of New York, Stony Brook, New York 11794-5215

Received February 10, 2004; Revised Manuscript Received May 6, 2004

ABSTRACT: The behavior of model-membrane-inserted polyLeu-rich peptides containing Asp residues located at various positions in their hydrophobic core was investigated. The topography of the bilayer-inserted α helices formed by these peptides was evaluated by measuring the emission λ_{max} and quenching the fluorescence of a Trp at the center of the peptide sequence. When Asp residues were protonated (at low pH), peptides that were incorporated into vesicles composed of dioleoylphosphatidylcholine (DOPC) adopted a topography in which the polyLeu sequence predominantly formed a normal transmembrane (TM) helix. When Asp residues were ionized (at neutral or high pH), topography was altered in a manner that would allow the charged Asp residues to reside near the bilayer surface. In DOPC vesicles, most peptides repositioned so that the longest segment of consecutive hydrophobic residues (12 residue minimum) formed a truncated/shifted TM structure. However, peptides with one or two charged Asp residues close to the center of the hydrophobic sequence and thus lacking even a 12-residue continuous hydrophobic segment, formed a helical non-TM state locating near the bilayer surface. At low pH, incorporation of the peptides into thicker bilayers composed of dierucoylphosphatidylcholine (DEuPC) resulted in the formation of a mixture of the normal TM state and the non-TM helical state located near the bilayer surface. In DEuPC vesicles at high pH, the non-TM state tended to predominate. How Asp-ionization-dependent shifts in helix topography may regulate the function of membrane proteins exposed to environments with differing pH in vivo (e.g., endosomes) is discussed.

The transmembrane (TM) segments of natural membrane proteins are commonly composed of hydrophobic α helices, 15−25 amino acids in length. The amino acid sequence of hydrophobic helices determines whether they will be TM, how they will be positioned within the lipid bilayer, and how they will interact with other membrane-inserted helices (*1*−*6*).

Although hydrophobic residues are predominant in TM helices, polar and ionizable ("charged") residues in such sequences are particularly important in determining helix behavior. In many cases, such hydrophilic residues are involved in TM helix−helix interactions (*7*, *8*). Presumably, the ability of hydrophilic residues to form hydrogen bonds (*2*, *9*) or salt bridges (*10*) with other membrane-inserted hydrophilic residues drives these interactions, while at the same time, alleviating some of the unfavorable energetics of inserting polar and ionizable residues within the bilayer.

The position of a hydrophilic amino acid in the primary sequence of a TM segment is an important parameter affecting helix−helix interactions. For example, it was recently shown that an Asn residue, which can strongly promote helix−helix interactions (*2*, *11*), significantly stabilized the trimerization of hydrophobic peptides in micelles when placed deeply in the hydrophobic core of the peptide, while an Asn near the edge of the hydrophobic sequence had little effect on oligomerization (*12*).

Hydrophilic residues can also alter the topography of membrane-inserted hydrophobic sequences by determining whether a TM or non-TM state forms. The introduction of too many charged or excessively hydrophilic residues can result in the formation of "semi-hydrophobic helices". Such helices can equilibrate between TM and non-TM states that lie close to the bilayer surface (*1*, *5*, *13*−*16*).

Even when a TM state is maintained in the presence of hydrophilic residues, they can alter the location of the TM sequence in the bilayer (*1*, *4*, *10*, *17*). In such cases, the position of hydrophilic residues in the primary sequence is again an important variable. von Heijne and colleagues showed that the residue forming the boundary of the inserted segment of a TM α helix derived from a leader peptidase could be altered by the introduction of single ionizable residues (i.e., Asp, Glu, Lys, and Arg) (*4*, *17*). Ionizable residues that were not too far from the end of the TM segment induced a shift in the position of one end of the sequence such that the charged residue would be located outside the hydrophobic core of the membrane.

We have studied the effect of hydrophilic residues upon the behavior of synthetic Lys-flanked polyLeu helices

† This work was supported by NIH Grant GM48596.

* To whom correspondence should be addressed. Phone: 631-632-8564. Fax: 631-632-8575. E-mail: erwin.london@stonybrook.edu.

‡ Department of Biochemistry and Cell Biology.

§ Department of Chemistry.

|| Current address: Department of Medical Biochemistry and Genetics, Texas A&M University, College Station, TX 77843.

10.1021/bi049696p CCC: $27.50
Published on Web 06/18/2004

incorporated into model membranes (*1*, *5*, *13*, *18*, *19*). The fluorescence of a Trp residue at the center of the polyLeu sequence was used to monitor helix behavior. It was found that in bilayers with near-physiological thickness the presence of a single uncharged hydrophilic residue near the center of the hydrophobic sequence was unable to disrupt TM topography (*1*). However, in thick bilayers, the cumulative effects of the presence of hydrophilic residues and negative mismatch (i.e., conditions in which the width of the hydrophobic core of the bilayer exceeds the length of the hydrophobic helix) resulted in the formation of a non-TM surface topography by a large fraction of the peptides. This state existed in equilibrium with the TM state. The extent of non-TM topography formation depended upon the type and number of substituting residues (*1*).

It was also found that a single charged Asp residue near the center of the hydrophobic sequence induced formation of the non-TM state (*5*, *19*). In contrast, two consecutive (and presumably charged) Lys residues near the center of the hydrophobic sequence tended to induce a shift in TM helix position rather than a non-TM state (*1*). This behavior was attributed to snorkeling, the ability of the membrane-inserted four-carbon Lys side chain to orient such that its amino group can be positioned near the bilayer surface (*20*−*22*) and thus allow burial of enough of the polyLeu sequence to form a stable truncated TM helix. Snorkeling effects have also been invoked to explain differences between the effects of Asp and Lys residues on the positioning of TM helices (*4*).

These findings were extended in this paper by examining the effect of the Asp position upon hydrophobic helix behavior. In vesicles with physiologically relevant bilayer widths, it was found that the fully TM state in which Asp residues were buried in the bilayer core predominated at low pH (where the Asp residues were uncharged), but that at high pH (where the Asp residues were charged) Asp residues could not be buried in the bilayer core and either a truncated TM helix formed or a shallowly located non-TM state formed, depending on the position of the Asp in the sequence.

EXPERIMENTAL PROCEDURES

Materials. Peptides $K_2GL_7DLWL_9K_2A$ [pL(D11)],[1] $K_2GL_6DL_2WL_9K_2A$ [pL(D10)], $K_2GL_5DL_3WL_9K_2A$ [pL(D9)], $K_2GLDL_7WL_9K_2A$ [pL(D5)], and $K_2GL_6DDLWL_9K_2A$ [pL(D10D11)] were purchased from the Research Genetics Division of Invitrogen (Huntsville, AL). $K_2GL_7DLWLDL_7K_2A$ [pL(D11D15)] was purchased from Anaspec Inc. (San Jose, CA). $K_2GL_3DL_5WL_9K_2A$ [pL(D7)] was purchased from Peptide Express, a division of BioExpress (Dublin, OH). The N termini of all of these peptides were acetylated, and the C termini were all amide-blocked. Phosphatidylcholines (1,2-diacyl-*sn*-glycero-3-phosphocholines) with even carbon number acyl chains (diC14:1Δ9cPC, dimyristoleoylphosphatidylcholine; diC16:1Δ9cPC; diC18:1Δ9cPC, dioleoylphosphatidylcholine, DOPC; diC20:1Δ11cPC; diC22:1Δ13cPC, dierucoylphosphatidylcholine, DEuPC; and diC24:1Δ15cPC) were purchased from Avanti Polar Lipids (Alabaster, AL). Lipids were stored in chloroform at −20 °C. The lipids used were shown to be pure by TLC. Synthetic peptides were further purified via reversed-phase HPLC using a C18 column with an 2-propanol/water gradient in which the solvents contained 0.5% (v/v) trifluoroacetic acid, starting at between 30 and 40% (v/v) 2-propanol (*23*). (In one case (pL(D11D15)) in which the peptide was sufficiently pure, a further purification step was omitted.) Peptide purity was checked using MALDI−TOF (Proteomics Center, Stony Brook University) and was estimated to be >90% in each case. (Tests of MALDI−TOF sensitivity to peptides with typical amino acid deletions found in impurities suggested that this value is a lower limit to the actual purity (data not shown).) Concentrations of purified peptides were measured by absorbance spectroscopy using a Beckman DU-650 spectrophotometer, using an ϵ for Trp of 5560 M^{-1} cm^{-1} at 280 nm. The peptides were stored at 4 °C in 1:1 (v/v) 2-propanol/water. Acrylamide was purchased from Sigma Chemical Co. (St. Louis, MO). A stock solution of 4 M acrylamide in water was used. 10-doxylnonadecane (10-DN) was custom-synthesized (contact authors for availability) by Molecular Probes (Eugene, OR). It was stored as a 4.2 mM stock solution [on the basis of a $\epsilon = 12$ M^{-1} cm^{-1} at 422 nm (*24*)] in ethanol at −20 °C.

Model Membrane Vesicle Preparation. Model membranes were prepared using the ethanol-dilution method (*5*, *13*). Peptides dissolved in 1:1 (v/v) 2-propanol/water and lipids dissolved in chloroform were mixed and then dried under a stream of N_2. Samples were then dried under high vacuum for 1 h. To make ethanol dilution vesicles, 10 μL (for 800-μL samples) or 30 μL (for 2-mL samples) of 100% ethanol was added to dissolve the dried peptide/lipid film. Then, 790 or 1970 μL of PBS (10 mM sodium phosphate and 150 mM NaCl, adjusted to pH 3.8 ± 0.1 with glacial acetic acid), respectively, was added to the samples while vortexing to disperse the lipid−peptide mixtures. Unless otherwise specified, final concentrations were 2 μM peptide and 200 μM lipid.

Fluorescence Measurements. Fluorescence data were obtained on a SPEX τ2 Fluorolog spectrofluorometer operating in the steady-state mode at room temperature. Measurements were taken on samples in semimicro quartz cuvettes (1-cm excitation path length and 4-mm emission path length) for most experiments. A 1-cm excitation and emission pathlength cuvette was used for pH titration experiments. A 2.5-mm excitation slit width and 5-mm emission slit width (band pass of 4.5 and 9 nm, respectively) were used for all experiments. Fluorescence emission spectra were measured over the range of 300−375 nm. Fluorescence from background samples containing the lipid but lacking the peptide was subtracted from the reported values. All measurements were taken at room temperature.

Measurement of λ_{max} in Bilayers of Differing Thickness. Samples with a peptide/lipid ratio of 1:100 were prepared as described above at pH 3.8 in a final volume of 800 μL. Samples were incubated for 1 h at room temperature before spectra were recorded. To adjust these samples to higher pH, 40−45 μL of 2.5 M Tris-base in water or 28 μL of 2 M

[1] Abbreviations: 10-DN, 10-doxylnonadecane; PC, phosphatidylcholine; DOPC, diC18:1Δ9cPC, dioleoylphosphatidylcholine; DEuPC, diC22:1Δ13cPC, dierucoylphosphatidylcholine; DQA, dual-quencher analysis; MALDI−TOF, matrix-assisted laser desorption ionization time-of-flight mass spectrometry; pL(D5), acetyl-$K_2GLDL_7WL_9K_2A$-amide; pL(D7), acetyl-$K_2GL_3DL_5WL_9K_2A$-amide; pL(D9), acetyl-$K_2GL_5DL_3WL_9K_2A$-amide; pL(D10), acetyl-$K_2GL_6DL_2WL_9K_2A$-amide; pL(D11), acetyl-$K_2GL_7DLWL_9K_2A$-amide; pL(D10D11), acetyl-$K_2GL_6DDLWL_9K_2A$-amide; pL(D11D15), acetyl-$K_2GL_7DLWLDL_7K_2A$-amide.

NaOH, was added (to obtain a final pH of ~8.5 (8.2−8.5) or 9.9, respectively. pH 9.9 was used for the pL(D11) peptide and pH ~8.5, for all of the other peptides). Spectra were remeasured after a further incubation at room temperature for about 1 h.

pH Titration Experiments. The 2-mL samples were prepared as described above. After the fluorescence emission intensity was measured at 330 and 350 nm (or emission λ_{max}), sample pH was increased by adding 1−8-μL aliquots of either 0.5 or 2 M NaOH while mixing. After addition of each aliquot of NaOH, samples were allowed to equilibrate for approximately 2 min before fluorescence was remeasured. Control experiments showed this to be a sufficient time for equilibration of pH across the bilayer (*18*, *19*) (data not shown). The total volume of NaOH added by the end of the titration experiment (at which pH was 11.4−11.6) was about 70 μL. Intensities were corrected for background fluorescence using controls lacking the peptide but were not corrected for the negligible level of dilution. The pH dependence of the ratio of fluorescence intensity at 350 nm and 330 nm (F_{350}/F_{330}) or λ_{max} was used to calculate pK_a values for the ionizable residues.

Acrylamide-Quenching Measurements. To quantify acrylamide quenching, fluorescence intensity and emission spectra were first measured in 800-μL samples containing model-membrane-incorporated peptides or background samples that were prepared at just low pH or at low pH and then adjusted either to pH ~8.5 or ~9.9 as described above. After incubation for roughly 1 h, a 50-μL aliquot of acrylamide from a 4 M stock solution dissolved in water was added. After a brief further incubation (about 5 min), fluorescence was remeasured. Fluorescence intensity was measured at an excitation wavelength of 295 nm and an emission wavelength of 340 nm. This excitation wavelength was chosen to reduce acrylamide absorbance (and the resulting inner-filter effect), and the emission wavelength was chosen to eliminate interference from the Raman band of water. Corrections to intensity were made both for dilution by the addition of acrylamide and for inner-filter effects (*24*). Fluorescence emission spectra were measured using an excitation wavelength of 280 nm. This excitation wavelength was chosen because the overall intensity was greater than when an excitation wavelength of 295 nm was used, despite the stronger inner-filter effect when 280 nm was used. Controls showed that emission spectra had very similar wavelength maxima using either excitation wavelength.

10-DN-Quenching Measurements. To measure the efficiency of 10-DN quenching, the fluorescence of samples (prepared as described above) in the absence of 10-DN was compared to that of samples containing 10-DN. To prepare the latter, samples containing model-membrane-incorporated peptides or background samples without the peptide were prepared as noted above, except that either 10 mol % (for DOPC) or 12 mol % (for DEuPC) of the lipid was replaced by an equivalent mole fraction of 10-DN. A larger fraction of the quencher was used in the DEuPC samples to maintain a constant ratio of doxyl groups to hydrophobic volume (*24*). Samples with and without 10-DN were prepared at pH 3.8, and then fluorescence intensity and emission spectra were measured. Sample pH was then raised to pH ~8.5 or ~9.9, as described above. After the samples were allowed to equilibrate at room temperature for about 1 h, fluorescence was remeasured. Fluorescence intensity was measured using an excitation wavelength of 280 nm and an emission wavelength of 330 nm. Emission spectra were recorded using an excitation wavelength of 280 nm.

Calculation of the Acrylamide/10-DN Quenching Ratio (Q Ratio). The ratio of quenching by acrylamide/10-DN was used to calculate Trp depth in the bilayer. This ratio was calculated from the formula Q ratio = $[(F_o/F_{acrylamide}) - 1]/[(F_o/F_{10-DN}) - 1]$, where F_o is the fluorescence of the sample with no quencher present and $F_{acrylamide}$ and F_{10-DN} are the fluorescence intensities in the presence of acrylamide or 10-DN, respectively (*24*).

Circular Dichroism (CD) Measurements. Circular dichroism spectra were recorded on a Jasco J-715 CD spectrophotometer at room temperature using a 1-mm path-length quartz cuvette. Samples were prepared at low pH as noted above with the exception that low pH-adjusted PBS diluted 10-fold with water (dilution had little effect on pH) was used to reduce solvent interference at low wavelengths. Control experiments using undiluted PBS showed similar spectral shapes but, in some cases, slightly stronger ellipticity (up to a 20% increase; G. A. Caputo and E. London, unpublished observations). After spectra were recorded at low pH, sample pH was raised using appropriate amounts of either Tris-base or NaOH to achieve pH values close to those used in the fluorescence experiments. Both low and high pH values were within 0.2−0.3 of those used in the fluorescence experiments. After incubation for about 1 h at room temperature, spectra were rerecorded. Reported spectra are the average of between 125 and 150 scans. Backgrounds from samples lacking peptide were subtracted. Overall, the α-helix content was estimated using three deconvolution programs: SELCON3 (*25*, *26*), CONTINLL (*27*), and CDSSTR (*28*). In most cases, the helix content computed by the three independent programs was consistent within ~10%. The averages of the values from the three programs are reported.

RESULTS

The behavior of model membrane-inserted Lys-flanked polyLeu peptides (pL peptides) containing one or two Asp substitutions at different positions in their primary sequence was studied. Including the Asp residue(s) and a Trp residue at the center of the hydrophobic sequence, the polyLeu-rich hydrophobic core of the peptides was 19 amino acids in length (20 amino acids if a flanking Gly residue is considered hydrophobic). This is sufficient to span the hydrophobic core of bilayers composed of DOPC. DOPC has 18 monounsaturated carbon fatty acyl chains and forms bilayers with a nonpolar core of approximately 30 Å in thickness, close to that expected for natural membranes (*29*).

Ionization Behavior of Asp Residues in the Core of Membrane-Inserted PolyLeu Peptides. The aim of this study was to characterize the topographical characteristics of model membrane-inserted Asp-containing peptides both when Asp residues were charged and uncharged. For this reason, pH titrations were performed to determine Asp pK_a values. The pH-dependent changes in ionization were detected by their effect on Trp emission (which is sensitive to ionization-induced changes in peptide topography, see below). Changes in the wavelength dependence of fluorescence emission were generally measured by the ratio of Trp emission intensity at

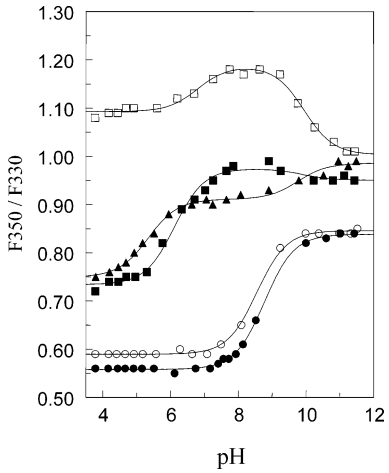

FIGURE 1: Effect of pH upon Trp fluorescence for Asp-containing polyLeu peptides incorporated in lipid vesicles. Samples were prepared at low pH and titrated with NaOH, while measuring the fluorescence after the addition of each aliquot. Peptide concentration was 2 μM, and lipid concentration was 200 μM. Curves are shown for (●) pL(D11) in DOPC vesicles, (○) pL(D11) in DEuPC vesicles, (■) pL(D9) in DOPC vesicles, (□) pL(D9) in DEuPC vesicles, and (▲) pL(D10D11) in DOPC vesicles. Single titrations are shown, but similar results were obtained with duplicate samples.

350 nm and 330 nm (F_{350}/F_{330}). This method is somewhat easier to use for titration experiments than the measurement of changes in the wavelength of maximum Trp emission (λ_{max}) (*18*, *19*). A low F_{350}/F_{330} value is equivalent to a blue-shifted Trp emission, and a high F_{350}/F_{330} ratio indicates a red-shifted emission.

Some representative pH titration curves are shown in Figure 1. In most cases, two distinct ionization events were observed as pH was increased. The first ionization event reflected Asp deprotonation and the second, deprotonation of the Lys residues that flank the hydrophobic sequence. In all cases, Asp ionization was accompanied by a red shift in Trp emission. Lys deprotonation was sometimes accompanied by a red shift but in other cases was accompanied by a blue shift. Controls were performed in a few cases to confirm that the fluorescence changes induced by increasing pH were reversible when pH was decreased (ref *19* and data not shown). Table 1 summarizes the pK_a values obtained from pH titrations for Asp-containing peptides incorporated in either DOPC vesicles or DEuPC vesicles. (DEuPC has 22 monounsaturated carbon fatty acyl chains.) In most cases, Asp pK_a fell in the pH range of 5−7 and Lys pK_a fell in the pH range of 9−11, both in DOPC and DEuPC bilayers (Table 1). The only striking exception was pL(D11). In agreement with previous results, the pL(D11) peptide only showed one ionization event near pH 8.5. This was previously identified as involving Asp deprotonation but may also involve simultaneous or nearly simultaneous Lys deprotonation (*19*).

It should be noted that similar Asp pK_a values were found for peptides in bilayers composed of dimyristoleoylphosphatidylcholine, a lipid with 14 carbon-atom monounsaturated acyl chains (data not shown). This confirms that pK_a values were not strongly dependent on the bilayer width. Therefore, for most subsequent experiments, pH 3.8 and 8.5 were used to study peptides in a state in which the Asp would be predominantly uncharged or charged, respectively. The flanking Lys residues should have remained at least largely charged at both of these pH values. To study the pL(D11) peptide under conditions in which the Asp residue was ionized, pH 9.9 was used.

Table 1: pK_a Values for Asp-Containing Peptides in DOPC or DEuPC Bilayers

	DOPC vesicles		DEuPC vesicles	
peptide	pK_{a_1} [a]	pK_{a_2}	pK_{a_1}	pK_{a_2}
pL(D5)	5.6 ± 0.04	9.2 ± 0.24	4.9 ± 0.2 [b]	11.2 ± 0.17 [b]
pL(D7)	6.7 ± 0.05	11.1 ± 0.06	7.1 ± 0.23	11.2 ± 0.07
pL(D9)	6.2 ± 0.06	9.8 ± 0.01	7.0 ± 0.33	10.5 ± 0.71
pL(D10)	6.1 ± <0.01	9.4 ± 0.11	5.6 ± 0.05	8.6 ± 0.45
pL(D11)	8.7 ± 0.05	*c*	8.6 ± 0.01	*c*
pL(D10D11)	5.3 ± <0.01	9.7 ± 0.08	4.2 ± 0.16; 6.2 ± 0.10 [d]	10.3 ± 0.80
pL(D11D15)	6.8 ± 0.04	9.2 ± 0.18	6.5 ± 0.06	8.9 ± 0.18

[a] pK_a values are the averages from titrations of duplicate samples. The range of averages is also shown. To estimate pK_a, points were fit to the equation for sigmoid or dual-sigmoid curves [using SlideWrite Plus for Windows version 6.00 (Advanced Graphics Software, Encinitas, CA)]. [b] Because of a red-shifted impurity, pK_a values for pL(D5) in DEuPC were calculated using changes in λ_{max}, rather than F_{350}/F_{330}. [c] No second pK_a was detected. [d] Data were fit to a triple-sigmoid equation. The two low pK_a values may arise from the separate ionization of the two Asp residues in pL(D10D11).

Principles of Distinguishing Topography of Bilayer-Inserted Hydrophobic Peptides through Fluorescence λ_{max} and Its Dependence Upon Bilayer Width. Next, Trp fluorescence was used to define the topography of the model-membrane-inserted peptides. It was previously shown that Trp emission λ_{max} could be used to estimate Trp depth and that when the Trp was placed in the center of the hydrophobic sequence λ_{max} could readily distinguish between TM and non-TM topographies (*1*, *5*, *19*). When in a fully TM orientation, the Trp locates at or near the bilayer center, which results in a very blue-shifted Trp emission λ_{max} in the range of 315−318 nm (*1*, *5*). If the peptide adopts a non-TM topography in which it locates close to the surface of the bilayer, the λ_{max} of Trp red-shifts strongly (e.g., to 335−340 nm). Intermediate values of λ_{max} are characteristic of either a combination of TM and non-TM topographies (*1*, *13*, *24*), or a shifted TM state in which only part of the polyLeu sequence forms a membrane-spanning segment and thus the Trp moves to an intermediate depth (*1*).

Additional studies demonstrated that the dependence of λ_{max} upon bilayer width/thickness could help distinguish between different topographical states (*1*). The most commonly observed case for polyLeu peptides with a very hydrophobic 19-residue core involves formation of a fully TM helix in normal-width DOPC bilayers (solid line of Figure 2). This gives highly blue-shifted fluorescence because the Trp is at the bilayer center. A red shift is observed for such peptides when they are incorporated into thicker bilayers. This red shift is due to the formation of an appreciable fraction of the non-TM surface state, in which the Trp is closer to the bilayer surface. This non-TM state forms because of negative mismatch; i.e., a situation in which the width of the hydrophobic core of the bilayer exceeds the length of the hydrophobic segment of a TM helix. In the TM state, this situation results in an energetically unfavorable burial of the hydrophilic residues flanking the hydrophobic sequence (*1*, *5*). There is also a red shift observed in very thin bilayers (i.e., under conditions of positive mismatch).

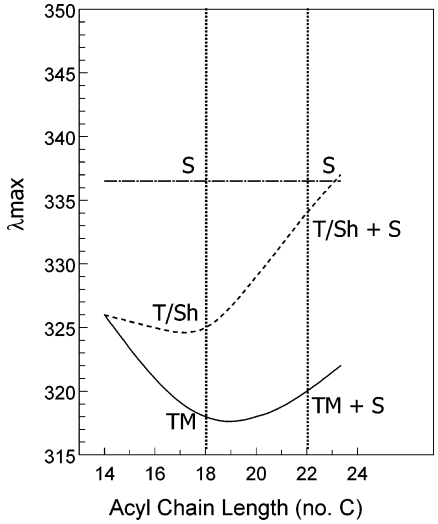

FIGURE 2: Schematic dependence of Trp λ_{max} upon lipid acyl chain length for polyLeu peptides adopting various membrane-associated topographies. The behaviors shown were previously identified for polyLeu peptides containing hydrophilic substitutions (*1*, *5*). (—) Typical λ_{max} behavior for a peptide with a central Trp residue and a hydrophobic length matching the acyl chain width for medium-width bilayers (18−20 carbon acyl chains). Fluorescence is highly blue-shifted in medium-width bilayers. In wider-width bilayers, a mixture of a TM and non-TM surface-located state forms and fluorescence red shifts. Red shift in thin membranes is due to oligomerization plus intrinsic bilayer-width effects (*5*, *13*). (- - -) λ_{max} behavior for a peptide that can form a truncated TM segment. Fluorescence in moderate-width bilayers is red-shifted relative to that for full-length TM helices because of the movement of Trp from the bilayer center in the shifted state. Formation of a non-TM surface-located state and additional red shifting occurs even in slightly wider bilayers. (-·-·-) Trp λ_{max} behavior for a peptide that adopts the non-TM surface-located state. Highly red-shifted fluorescence is observed in bilayers of any thickness. In all cases, typical λ_{max} values are shown; however, depending on the exact Trp depths and any interactions between Trp and polar residues, λ_{max} values in a specific topography can be different than the values shown (see the text for details).

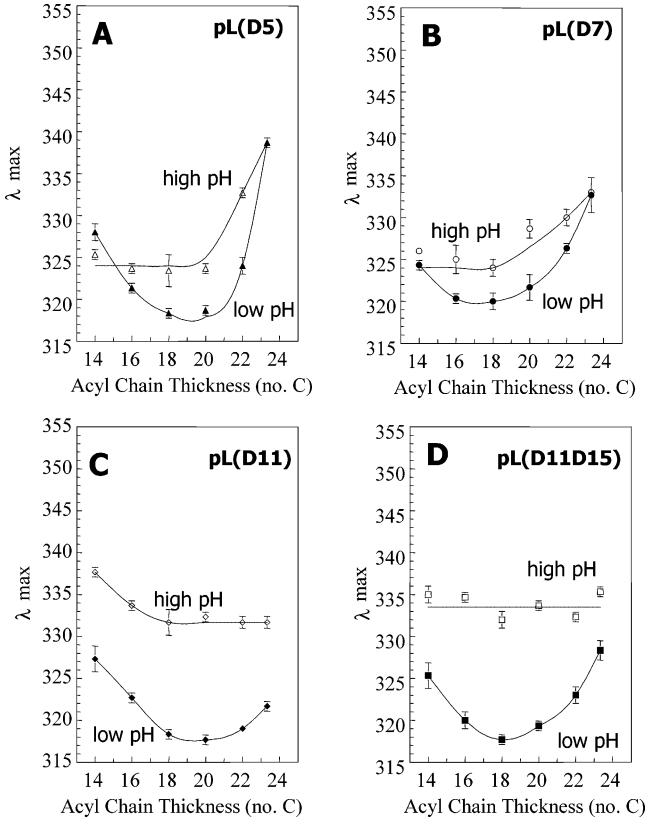

FIGURE 3: Effect of lipid acyl chain length on Trp emission λ_{max} of Asp-containing polyLeu peptides incorporated into phosphatidylcholine vesicles. Peptides studied were (A) pL(D5), (B) pL(D7), (C) pL(D11), and (D) pL(D11D15). Filled symbols indicate λ_{max} values at conditions in which Asp was protonated (pH 3.8), and open symbols indicate λ_{max} values from the same samples under conditions in which Asp was charged, i.e., after raising pH to 8.3−8.5 [for pL(D7), pL(D5), and pL(D11D15)] or pH to ∼9.9 [for pL(D11)]. Samples contained 2 μM peptide and 200 μM lipid dispersed in pH-adjusted PBS. The lipids that were used all had monounsaturated acyl chains. Reported values are the average from three to six samples.

This appears to be due to a combination of the formation of TM oligomers (*13*) and the fact that even a Trp at the bilayer center is closer to the bilayer surface in thin bilayers than in thicker bilayers (*5*). Overall, a "U" shaped curve for λ_{max} versus the bilayer thickness curve is observed.

A second case previously observed is that of peptides that when incorporated in DOPC bilayers form a shifted TM state, in which only a truncated segment of the polyLeu sequence forms a TM helix (*1*). This shifted state forms so that a hydrophilic residue within the hydrophobic sequence can reside near the bilayer surface. The shifted state exhibits not only more red-shifted fluorescence in DOPC (because of its Trp being shifted from the center of the bilayer), but also more sensitivity to negative mismatch (dashed line of Figure 2). This increased sensitivity is expected because the shorter the TM segment the greater the degree of negative mismatch at any specific bilayer width. The resulting pattern of λ_{max} versus bilayer thickness will be referred to as a "J" curve.

The final case previously observed is that of peptides forming a non-TM helix near the bilayer surface in DOPC (*1*). This has been observed for polyLeu sequences that are not hydrophobic enough to form a TM helix because of the presence of too many hydrophilic substitutions within the polyLeu core. Because in this state the peptides only interact with one leaflet of the bilayer, their topography is largely unaffected by bilayer width. Thus, they show red-shifted Trp fluorescence that is insensitive to bilayer width (dashed-dotted line of Figure 2) (*1*).

Topography of Asp-Containing PolyLeu Peptides at Low and High pH. The analysis described above was used to evaluate the effect of bilayer width upon Trp λ_{max} of Asp-containing peptides both under low pH conditions, in which the Asp would be protonated, and under higher pH conditions, in which it would be deprotonated (i.e., charged). Figure 3 shows the effect of bilayer thickness on λ_{max} for four Asp-containing peptides: pL(D5), pL(D7), pL(D11), and pL(D11D15). At low pH, all four peptides exhibited typical U-shaped curves with highly blue-shifted fluorescence in bilayers of intermediate width (filled symbols of Figure 3). As noted above, this is characteristic of peptides for which the entire hydrophobic polyLeu sequence participates in a TM helix at intermediate bilayer widths and for which a mixture of TM helix and a non-TM surface topography forms in thicker bilayers.

When the pH in these samples was increased to a value where the Asp is ionized, peptide λ_{max} red-shifted in all cases (open symbols of Figure 3). This implies that the Trp moved to a shallower depth because the charged Asp residue moved toward the bilayer surface. The exact behavior observed

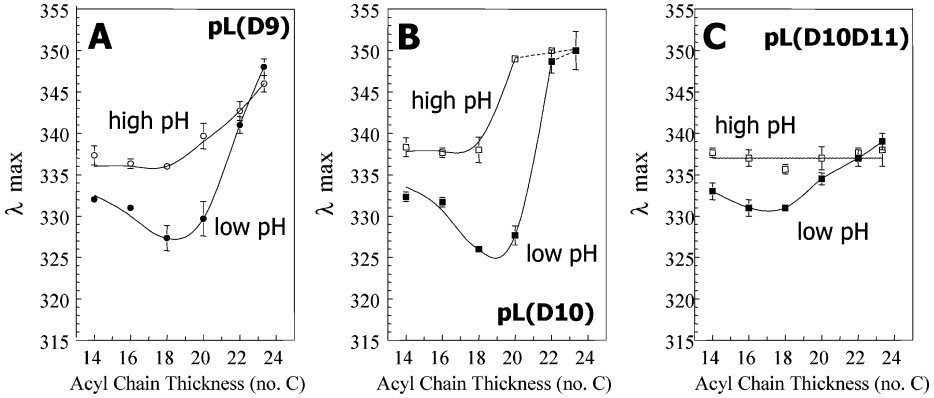

FIGURE 4: Effect of lipid acyl chain length on Trp emission λ_{max} of Asp-containing polyLeu peptides incorporated into phosphatidylcholine vesicles. (A) pL(D9), (B) pL(D10), and (C) pL(D10D11). Filled symbols indicate λ_{max} values obtained under conditions in which Asp was protonated (pH 3.8), and open symbols indicate λ_{max} values for the same samples under conditions in which Asp was charged (after raising pH to 8.2−8.5). The dashed line for pL(D10) is an approximation. In this case, λ_{max} values when fluorescence was red-shifted were affected by the presence of a red-shifted impurity. Reported values are the average obtained from three to six samples. Experimental conditions are the same as in Figure 3.

depended upon the Asp residue position. The pL(D11) and pL(D11D15) peptides both exhibited strongly red-shifted Trp λ_{max} values in all bilayer widths. This indicates that when the Asp was ionized these two peptides adopted the shallow non-TM topography at all bilayer widths. In contrast, pL(D5) and pL(D7) at high pH exhibited a red-shift profile with a J-type dependence of λ_{max} upon bilayer width. This behavior indicates that the pL(D5) and pL(D7) peptides formed truncated/shifted helices in DOPC bilayers and either the non-TM topography or a mixture of the truncated TM and non-TM topography in wider bilayers.

Figure 4 shows the effect of bilayer thickness on three additional Asp-containing peptides, pL(D9), pL(D10), and pL(D10D11). At low pH, these peptides exhibited U-type width-dependence profiles similar to the peptides shown in Figure 3. However, Trp emission λ_{max} values at low pH were considerably red-shifted at all bilayer widths relative to those for the peptides studied in Figure 3. This red shift was likely to be due to direct Trp−Asp interactions. These peptides have Asp residues in positions (9 and 10) that can directly interact with the Trp one helical turn away (at position 13). Using bilayer-inserted peptides, it was previously observed by Jones and Gierasch that when Trp and Asp are in close proximity Trp fluorescence is strongly red-shifted (*16*). At high pH, Figure 4 shows that all of these peptides exhibited fluorescence that is even more strongly red-shifted than at low pH. This behavior again indicates that ionized Asp residues locate closer to the bilayer surface than uncharged Asp. The pL(D9) and pL(D10) peptides showed a J-type dependence of λ_{max} upon bilayer width, while pL(D10D11) exhibited highly red-shifted Trp emission that was relatively insensitive to bilayer width. The most likely explanation of these results is that in DOPC vesicles at low pH pL(D9), pL(D10), and pL(D10D11) adopted the normal TM state, while in DOPC vesicles at high pH, pL(D9) and pL(D10) formed truncated/shifted helices and pL(D10D11) formed the non-TM state. In thicker bilayers, all of the peptides appeared to form predominantly the non-TM state.

Dependence of Trp Depth Upon Bilayer Thickness at Low and High pH. Because λ_{max} can be sensitive to factors other than Trp depth, dual-quencher analysis (DQA) was used to confirm topographical assignments by measuring Trp depth more directly. The DQA method utilizes two quenchers of Trp fluorescence, acrylamide and 10-DN, to assess Trp depth. Acrylamide significantly quenches Trp residues that are at or near the membrane surface, while 10-DN strongly quenches Trp residues that are buried in the nonpolar core of the bilayer. The ratio of acrylamide quenching to 10-DN quenching (Q ratio) has been shown to respond nearly linearly to Trp depth in the bilayer, such that a low quenching ratio indicates a deeply located Trp, while a high Q ratio is indicative of a Trp located at or near the bilayer surface (*1*, *24*). Similar to the situation for intermediate λ_{max} values, intermediate Q ratios can arise either from peptides that adopt multiple bilayer-associated conformations with different Trp depths or from peptides that adopt a shifted TM conformation with an intermediate Trp depth (see below).

Table 2: Quenching of Membrane-Inserted Peptide Trp Residues by Acrylamide and 10-DN at Low and High pH

	low pH		high pH	
peptide	acrylamide	10-DN	acrylamide	10-DN
	F_o/F[a] Values for Peptide Quenching in DOPC			
pL(D5)	1.12 ± 0.01	3.13 ± 0.07	1.16 ± 0.01	2.13 ± 0.08
pL(D7)	1.13 ± 0.03	2.60 ± 0.04	1.13 ± 0.02	2.02 ± 0.05
pL(D9)	1.18 ± 0.01	3.67 ± 0.28	1.45 ± 0.03	1.41 ± 0.09
pL(D10)	1.22 ± 0.02	2.90 ± 0.22	1.39 ± 0.08	1.58 ± 0.03
pL(D11)	1.13 ± 0.01	3.30 ± 0.31	1.25 ± 0.01	2.05 ± 0.08
pL(D10D11)	1.35 ± 0.04	2.31 ± 0.18	1.45 ± 0.01	1.40 ± 0.07
pL(D11D15)	1.14 ± 0.02	3.56 ± 0.08	1.36 ± 0.02	3.20 ± 0.17
	F_o/F Values for Peptide Quenching in DEuPC			
pL(D5)	1.35 ± 0.02	2.51 ± 0.26	1.43 ± 0.08	1.84 ± 0.02
pL(D7)	1.21 ± 0.02	1.62 ± 0.03	1.24 ± 0.01	1.50 ± 0.06
pL(D9)	1.74 ± 0.04	1.63 ± 0.01	1.71 ± 0.05	1.45 ± 0.07
pL(D10)	1.67 ± 0.01	1.53 ± 0.22	1.60 ± 0.03	1.46 ± 0.10
pL(D11)	1.34 ± 0.01	2.06 ± 0.03	1.49 ± 0.14	2.45 ± 0.10
pL(D10D11)	1.56 ± 0.07	1.65 ± 0.04	1.51 ± 0.05	1.38 ± 0.06
pL(D11D15)	1.20 ± 0.01	2.96 ± 0.14	1.38 ± 0.02	2.82 ± 0.09

[a] F_o/F is the ratio of fluorescence in the absence of the quencher to that in the presence of the quencher. The average of values obtained from three to six samples and the standard deviation of the average are shown. Low pH = 3.8; high pH ∼ 8.5 or 9.9 for pL(D11).

Quenching data for individual quenchers is shown in Table 2. Quenching was affected by both Trp position and Asp charge and generally shows the expected inverse correlation between acrylamide quenching and 10-DN quenching. Figure 5 shows the Q ratios calculated from these data. Figure 5A shows Q ratios for the series of Asp-containing peptides at

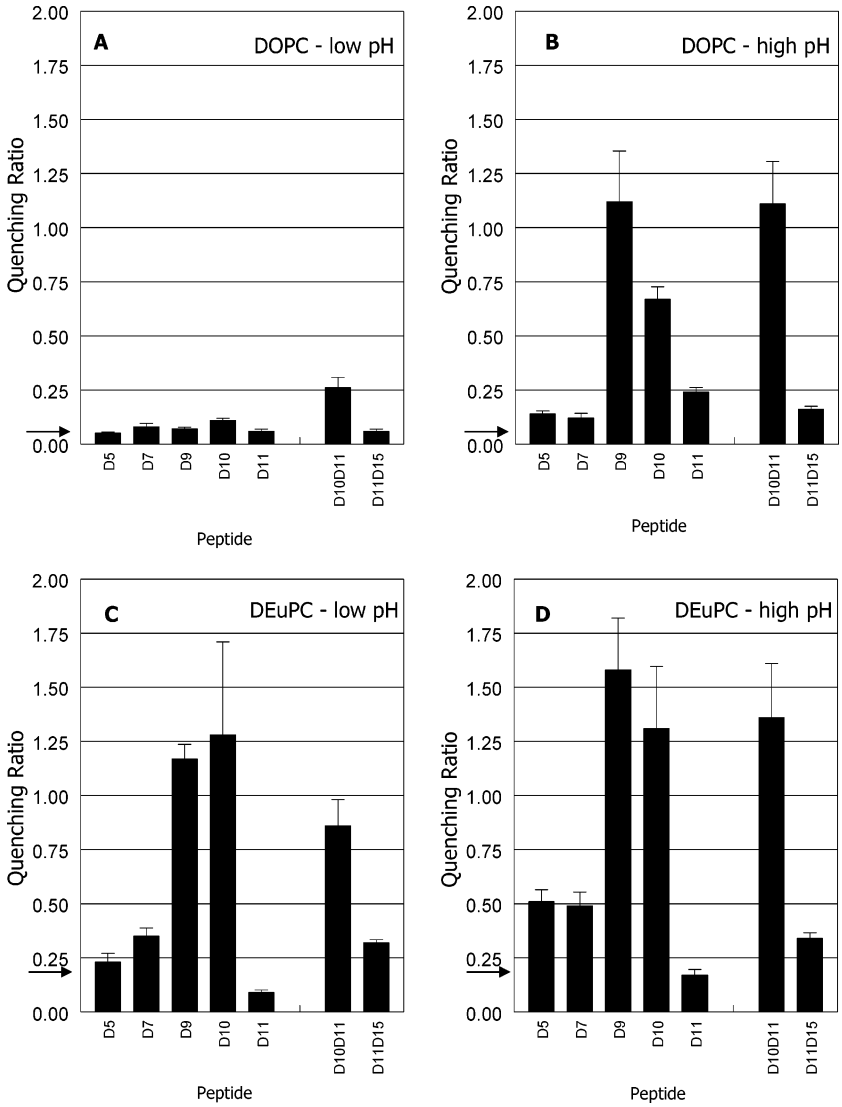

FIGURE 5: Q ratios for Asp-containing polyLeu peptides incorporated into lipid vesicles. (A) Q ratio for peptides in DOPC vesicles at pH 3.8. (B) Q ratios for peptides in DOPC vesicles at pH ~8.5 or [for pL(D11)] at pH ~9.9. (C) Q ratios for peptides in DEuPC vesicles at pH 3.8. (D) Q ratios for peptides in DEuPC vesicles at pH ~8.5 or [for pL(D11)] at pH ~9.9. Average values and standard deviations obtained from three to six samples are shown. Arrows adjacent to the *y* axes show the Q ratio for a case in which previous studies show Trp locates at the bilayer center, a polyLeu-peptide-lacking Asp (*24*). The *x* axis identifies the peptide by Asp position in the peptide sequence. Sample conditions are the same as in Figures 3 and 4, except that samples containing 10-DN had a lipid composition of 90 mol % DOPC plus 10 mol % 10-DN or 88 mol % DEuPC and 12 mol % 10-DN.

low pH when incorporated in DOPC vesicles. Consistent with the λ_{max} data, under these conditions, all of the peptides exhibited very low Q ratios, indicative of deeply located Trp.

In Figure 5B, the Q ratios are shown for the peptides in DOPC vesicles at high pH. Overall, the Q ratios increased when compared to the corresponding low pH values. This is consistent with the red shifts observed in λ_{max} and the conclusion that peptide topography at high pH changed either to a non-TM surface state or truncated/shifted TM helix. However, the increase in Q ratios varied quite widely, with the highest Q ratios observed for the pL(D9), pL(D10), and pL(D10D11) peptides. In the cases of pL(D5) and pL(D7), the relatively small change in the Q ratio can be explained by the fact that the Asp was close to the end of the hydrophobic sequence, and even upon formation of the truncated/shifted state the Trp should remain relatively deeply buried. On the other hand, pL(D11) and pL(D11D15), two of the peptides assigned to shallow surface conformations based on their λ_{max} values and the response of λ_{max} to bilayer thickness, also surprisingly exhibited relatively low Q ratios (see explanation below).

In Figure 5C, Q ratios are shown for the peptides in DEuPC vesicles at low pH. Overall, the Q ratios again showed an increase relative to the corresponding values in DOPC at low pH, in agreement with the red shifts observed in λ_{max} and the conclusion that peptide topography changed to a mixture of the normal TM and non-TM surface states under these conditions. Again, however, the increase in Q ratios varied quite widely, with the highest Q ratios observed for the pL(D9), pL(D10), and pL(D10D11) peptides.

In Figure 5D, the Q ratios are shown for the peptides in DEuPC vesicles at high pH. Overall, the Q ratios were increased when compared to any of the other conditions. This is in agreement with observation that red shifts in λ_{max} were the largest in this condition and the conclusion that the peptides were predominantly in a non-TM surface topography. Nevertheless, once again, a wide variation in Q values for different peptides was observed.

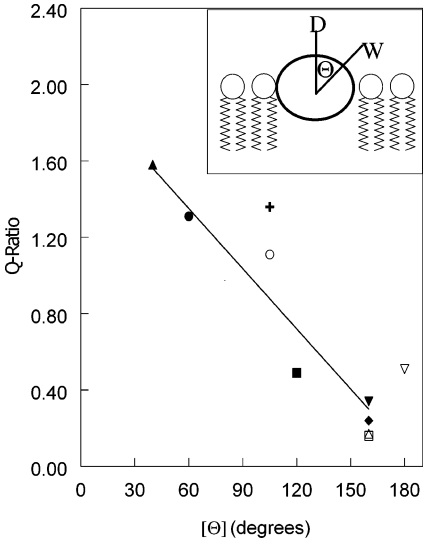

FIGURE 6: Correlation between quenching and the angle between Asp and Trp: dependence of Q ratios upon the estimated angle (Θ) between Trp and Asp side-chain α carbons under conditions in which peptides predominantly form non-TM structures at high pH as judged by λ_{max} behavior. Points are shown for peptides in DOPC vesicles for (△) pL(D11), (○) pL(D10D11), and (□) pL(D11D15). Points are shown for peptides in DEuPC vesicles for (▽) pL(D5), (■) pL(D7), (▲) pL(D9), (●) pL(D10), (◆) pL(D11), (+) pL(D10D11), and (▼) pL(D11D15). The line shown represents a least-squares linear fit (correlation coefficient = 0.76) Inset: Schematic representation of an end-on view of a surface-oriented peptide showing the definition of Θ. For peptides containing two Asp residues, Θ was defined as the angle between the Trp and the average direction of the individual Asp residues.

Correlation of Q Ratios to the Position of the Trp Residue Relative to the Asp Residue. It was initially puzzling that peptides that seemed to locate shallowly in the bilayer as judged by λ_{max} criteria showed relatively deep Trp depths as judged by the Q ratio. One possible explanation was that the Q ratio in the shallowly located non-TM state was strongly dependent on whether the Trp was on the side of the helix facing the aqueous solution or on the side facing the interior of the bilayer. This factor has a large effect on the depth of a residue in a non-TM state (*47*). It should depend on the position of the Trp relative to the Asp residue. A reasonable assumption is that in the non-TM state peptides tend to orient so that the Asp will be as far from the bilayer core as possible, that is, with the Asp facing the aqueous environment. Combined with the fact that the peptides were largely α helical (see below), this allows an estimation of the Trp side-chain location in the non-TM state. The angle between the Asp side chain and the Trp side chain (Θ) was calculated using the values for an ideal α helix (in which a one-residue difference in position is equivalent to a Θ of 100°).

A graph of Q ratio versus Θ is shown in Figure 6 for peptides under conditions in which they appeared predominately to adopt the non-TM shallow surface conformation (as judged by the λ_{max} experiments). A fairly strong linear correlation between Θ and Q ratio can be seen from these data. It is noteworthy that the peptides that exhibited anomalously low Q ratios, pL(D11) and pL(D11D15), also had Θ values close to the maximum of 180°, i.e., with the Asp on the exact opposite side of the helix relative to the Trp. This strongly suggests that, even when such peptides were at the surface of the bilayer, they were oriented so that the Trp was facing directly into the core of the bilayer, resulting in a deep Trp location. In contrast, peptides with the smallest Θ were those that exhibited the largest Q ratios in the non-TM state. These results indicate that when non-TM states are present Q ratio measurements *by themselves* can be deceptive and that topographies defined by the λ_{max}/bilayer-width experiments are less likely to be misleading (see the Discussion).

Detection of Multiple Peptide Populations by Quencher-Induced Shifts in Trp λ_{max}. Given the above-outlined complications arising from the position of Trp relative to that of Asp, an additional method to distinguish a shifted/truncated TM state from a mixture of deep and shallowly located states was needed to confirm our topographical assignments. These cases are the most difficult to distinguish from each other because, as noted above, an intermediate λ_{max} and intermediate Q ratio can arise from either of these situations (*1*, *24*).

To distinguish between these possibilities, the heterogeneity of Trp depth was analyzed using fluorescence quenching. When a bilayer-inserted peptide adopts multiple conformations with different Trp depths, its Trp emission will be a composite of the emission spectra of the different populations. In such cases, it was shown previously that acrylamide will preferentially quench the shallow population, from which the more red-shifted emission would normally arise (*1*, *24*). This results in an overall blue shift of the Trp emission spectrum. Conversely, 10-DN preferentially quenches the deeper population and thus induces a red shift in the Trp emission spectrum (*1*, *24*). If instead, only one population with an intermediate Trp depth is present, then the quenchers induce very little or no shift in λ_{max} (*1*).

Table 3 shows λ_{max} values for the model-membrane-inserted Asp-containing poly-Leu peptides and how they were affected by the presence of acrylamide or 10-DN. When incorporated in DOPC bilayers at low pH, the combination of blue-shifted emission and small quencher-induced λ_{max} shifts confirms that all of the peptides predominantly adopt one conformation with the Trp near the bilayer center. When incorporated in the thicker DEuPC bilayers at low pH, the peptides show not only the above-described red shift in the absence of the quencher, but also the large quencher-induced shifts in λ_{max} of the type predicted for a heterogeneous mixture of TM and non-TM surface-located topographies. In contrast, although at high pH, in DOPC vesicles, Trp emission is also red-shifted relative to that in DOPC vesicles at low pH, the quencher-induced shifts are much smaller. This is consistent with a single population of peptides with an intermediate Trp depth, i.e., a shifted TM topography. Because these conclusions agree with those obtained from the values of λ_{max} as a function of bilayer width in the absence of the quencher (Figures 2−4), they confirm the assignments of the topography of the Asp-containing peptides. (It should be noted that the quencher-induced shifts in DEuPC vesicles at high pH were generally less than those at low pH (data not shown). In combination with the observation that Trp depths were the shallowest in DEuPC vesicles at high pH, this supports the conclusion that, when Asp was ionized and negative mismatch was strong, the surface form tended to predominate.)

Asp-Containing PolyLeu Peptides Are α-Helical at Low and High pH. Previous studies showed that bilayer-inserted

Table 3: Quencher-Induced Shifts in Trp Emission λ_{max} for Membrane-Inserted Peptides in DOPC or DEuPC Vesicles

peptide	lipid	pH	λ_{max} (nm)[a]	λ_{max} (nm) acrylamide	λ_{max} (nm) 10-DN	|total shift| (nm)[b]
pL(D5)	DOPC	3.8	318.3	319	318	**1.0**
	DEuPC	3.8	324	319.7	332.7	**13.0**
	DOPC	8.5	323	323	325.3	**2.3**
pL(D7)	DOPC	3.8	320	319.7	320	**0.3**
	DEuPC	3.8	326.3	326.7	331	**4.3**
	DOPC	8.5	324	*c*	325.3	***c***
pL(D9)	DOPC	3.8	327.3	327	330.7	**3.7**
	DEuPC	3.8	341	335	345.7	**10.7**
	DOPC	8.5	336	334	336	**2.0**
pL(D10)	DOPC	3.8	326.8	327.1	326.3	**0.8**
	DEuPC	3.8	348.7	342	349.7	**7.7**
	DOPC	8.5	337.6	338.2	340.3	**2.1**
pL(D11)	DOPC	3.8	318.7	318	317.3	**0.7**
	DEuPC	3.8	317.7	318	319.3	**1.3**
	DOPC	9.9	332.3	330.7	332.3	**1.6**
pL(D10D11)	DOPC	3.8	331	329.7	330.7	**1.0**
	DEuPC	3.8	337	334.3	340	**5.7**
	DOPC	8.5	335.7	336.3	337	**0.7**
pL(D11D15)	DOPC	3.8	317.7	318	319	**1.0**
	DEuPC	3.8	323	319.3	328	**8.7**
	DOPC	8.5	331.7	333.7	337	**3.3**

[a] Reported λ_{max} values are averages from three to six samples. In general, λ_{max} values were reproducible to within ±1 nm. [b] Total shift is absolute value of the difference between the λ_{max} in the presence of 10-DN and λ_{max} in the presence of acrylamide. [c] Samples contained varied amounts of a red-shifted impurity that made λ_{max} determination and shift calculation impossible.

polyLeu peptides with various hydrophilic substitutions maintain α-helical secondary structure. To determine whether the peptides used in this study maintained a predominantly α-helical structure, CD spectra of bilayer-inserted Asp-containing peptides were measured. For each peptide, CD spectra were recorded for peptides incorporated in both DOPC and DEuPC bilayers and at both pH values both above and below the Asp pK_a values. All peptides gave spectra with the characteristic shape and intensities of α-helix-rich polypeptides (Figure 7). Analysis of helical content (see the Experimental Procedures) confirmed that the peptides formed highly helical structures under all conditions studied. Averaging over all peptides, there was no significant overall difference between helix content in DOPC vesicles (77 ± 4%) and DEuPC vesicles (73 ± 1%) or between samples at low pH (76 ± 3%) and the same samples after adjustment to high pH (74 ± 2%).

DISCUSSION

Uncharged and Charged Asp Residues Have Very Different Effects on the Behavior of Hydrophobic Helices. Figure 8 summarizes the behavior observed for Asp-containing polyLeu peptides. At low pH in the absence of hydrophobic mismatch, these peptides form TM helices such that the uncharged Asp residue remains buried within the bilayer regardless of its position in the helix (upper left panel of Figure 8). At low pH in the presence of negative mismatch, mixtures of TM and non-TM topographies tend to form, with the degree of non-TM topography formation somewhat exceeding that for polyLeu peptides lacking an Asp (*1*) (lower left panel of Figure 8). From comparison to earlier studies it appears that a protonated Asp destabilizes TM topography to a degree similar to that of other polar, uncharged residues (*1*). Because whether Asp and Trp are on the same side of a helix affects both λ_{max} and Q ratio, it was difficult to detect an effect of varying Asp position on the stability of the TM state when Asp residues are uncharged. Nevertheless, it can be stated that the exact

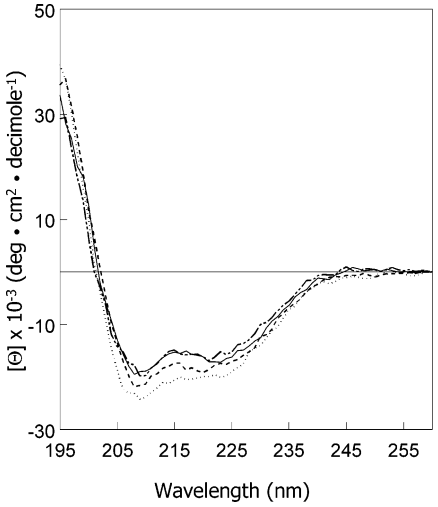

FIGURE 7: CD spectra of pL(D11D15) peptide incorporated in lipid vesicles. pL(D11D15) in (—) DOPC vesicles at pH 3.8, (- - -) DOPC vesicles at pH 8.2, (••••) DEuPC vesicles at pH 3.8, and (-••-) DEuPC vesicles at pH 8.2. Samples were prepared at pH 3.8, CD spectra were recorded, sample pH was raised to pH 8.2, and after an incubation of approximately 1 h spectra were re-recorded. Helix content for pL(D11D15) (calculated as described in the Experimental Procedures) and standard deviations for values from three different helix calculation programs were 72 ± 7% in DOPC at low pH, 68 ± 7% in DOPC at high pH, 73 ± 3% in DEuPC vesicles at low pH, and 62 ± 6% in DEuPC vesicles at high pH. Peptide concentration was 2 μM, and lipid concentration was 200 μM. The other peptides used in this study exhibited CD spectra with similar shapes and intensities.

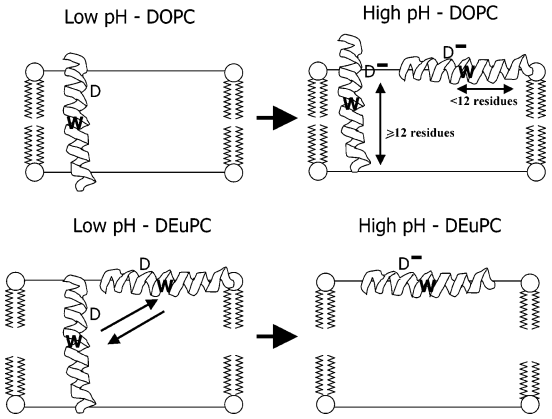

FIGURE 8: Schematic illustration of Asp-containing poly-Leu peptide behavior in lipid bilayers under different conditions. In DOPC vesicles at low pH, all of the peptides studied form a fully TM sequence with the protonated Asp buried in the bilayer and a Trp at the bilayer center. At low pH in DEuPC vesicles, the peptides exhibit an equilibrium between the fully TM topography and a non-TM surface topography with a displaced Trp depth because of the negative mismatch. At high pH in DOPC vesicles, Asp residues are charged and the peptides form either the truncated TM helices or the non-TM surface topography to move the charged Asp out of the bilayer core. Both of these states shift the Trp position away from the bilayer center. The truncated TM topography predominates when the length of the longest Leu-rich segment uninterrupted by charged Asp is at least 12 residues long. At high pH in DEuPC vesicles, the non-TM surface topography predominates because of the combination of the presence of charged Asp residues and strong negative mismatch.

position of protonated Asp residues in the sequence did not seem to have a critical effect on the stability of the TM state. This is shown by the observation that for almost all sequences at low pH bilayer a strong red shift, indicative of increased formation of the non-TM state, was only observed in samples in which lipid acyl chains were 22 or more carbon atoms long. However, for pL(D10D11), there are hints of a decreased stability of the TM state at low pH relative to peptides with one Asp or one with two nonconsecutive Asp (pL(D11D15)) as judged by a mismatch-related increase in red shift in bilayers with 20 carbon fatty acyl chains and by a slightly elevated Q ratio in DOPC (see the Results).

Experiments at higher pH showed that the effect of charged Asp residues on helix topography is more dramatic than the effect of uncharged Asp. It was previously concluded that a charged Asp residue close to the center of the sequence of a hydrophobic polyLeu helix would locate at the bilayer surface and abolish the ability of a polyLeu helix to form a TM state (*19*). From the results in this study, it appears that an analogous inability to bury deep within the bilayer is true for charged Asp residues positioned anywhere in a hydrophobic sequence. If the Asp position is close enough to one end of the sequence such that there is a residual segment of 12 or longer consecutive hydrophobic residues, then in DOPC bilayers (which are about as wide as natural membrane bilayers) this residual hydrophobic segment will form a truncated TM helix allowing the Asp residue to be positioned close to the bilayer surface (upper right panel of Figure 8). Because the TM sequence is truncated, its stability in the TM state is less than that of a full-length TM helix. This results in a greater tendency to form the non-TM topography when bilayer width is increased relative to that when Asp is protonated (bottom panels of Figure 8).

If a charged Asp residue is close to the peptide center, so that the largest consecutive hydrophobic sequence in the peptide is less than 12 residues, then the non-TM form predominates even in DOPC bilayers (top right panel of Figure 8). This too can be thought of as being a consequence of negative mismatch between the truncated hydrophobic sequences and bilayer width. For a short hydrophobic sequence, even insertion in DOPC bilayers can be a case of negative mismatch.

An expected consequence of forming a truncated TM helix would be a significant shift in the helix position in terms of which residues are at the center of the bilayer and which are at the bilayer surface. The observation of decreased Trp depth upon Asp ionization is consistent with this behavior (see the Results). A local thinning of the bilayer such that the Asp residue is closer to the bilayer surface may also occur. The short hydrophobic segment, which is separated from the truncated TM segment by the charged Asp, may either protrude into an aqueous solution (as shown in the top right panel of Figure 8) or might bend over and associate with the bilayer surface. A bend would likely involve a break in the helix structure, but a decrease in helix content was not detected in the CD spectra reported here under conditions in which the TM segment appeared to be truncated, perhaps because CD is insufficiently sensitive to the small change in secondary structure that would be involved.

The tendency of bilayer-inserted Asp residues to remain uncharged should not be over-generalized. An Asp residue within the core of a multi-helix protein but exposed to a local polar environment might be charged, even if located close to the bilayer center in depth. It is also possible that a lipid-exposed Asp may be charged when in a shallowly inserted location in the bilayer.

It should also be noted that when a hydrophobic helix is longer than necessary to span the lipid bilayer the movement of an Asp residue within the hydrophobic sequence to the proximal bilayer surface because of ionization could result in a loss of helix tilt such that the distal boundary of the inserted segment is unaltered rather than a shift in the position of the entire helix relative to the bilayer (*30*). Polypeptides that have relatively short-length TM segments, like those studied in this paper, could not reposition in this fashion.

Analyzing Topography from Fluorescence Parameters. In this paper, a *combination* of fluorescence-based techniques was employed to assay hydrophobic helix topography in bilayers. This was critical to circumvent ambiguities in interpretation of individual fluorescence parameters. Because λ_{max} of Trp emission is sensitive to polarity, it is sensitive to Trp depth in bilayers (*1*, *5*, *13*, *19*). Using a Trp at the center of a hydrophobic sequence, it was previously shown that a TM orientation results in an extremely blue-shifted λ_{max}, while in the shallow non-TM topography, λ_{max} is red-shifted. However, it was also found that oligomerization could red-shift λ_{max} (*13*, *18*). In the present study, the red shift caused by Asp "interaction" with Trp was an additional complicating factor. This was not unexpected because, as noted above, Trp red shifts were previously found for Asp and Trp in neighboring positions in a membrane-inserted hydrophobic peptide (*16*).

For these reasons, the recently introduced DQA was chosen to more directly measure the Trp depth (*24*). In most cases, this was sufficient to confirm topographic assignments from λ_{max}. However, we identified a novel ambiguity that can arise in depth measurements when a helix adopts a non-TM surface location. The troublesome case was when a peptide sequence is such that in the non-TM state the Trp faces the bilayer core. In this situation, a relatively deep Trp depth (low Q ratio) is observed even though the peptide itself is close to the bilayer surface. In the extreme examples in which the Trp in a non-TM peptide was probably facing toward the bilayer center (i.e., pL(D11) and pL(D11D15) peptides), Q ratios were indicative of deep Trp depth even though λ_{max} was somewhat red-shifted. We speculate that this difference reflects an anomalously low Q ratio arising from two factors. First, the peptide may sterically shield the Trp from the aqueous quencher acrylamide. Second, in the non-TM state, the peptides should sterically push lipids away, creating a space directly underneath the peptide that is relatively difficult to fill with lipid acyl chains. The hydrophobic 10-DN molecule may tend to fill in this space such that there is an excess of 10-DN directly under the peptide and thus close to the Trp. [A similar phenomenon may explain the unusually deep Trp depth that we previously measured for pL(D11) at high pH using parallax analysis (*19*)]. In future studies, changing the position of the Trp in the sequence by one or two residues may avoid these complications.

Whatever the explanation, it was desirable to use additional criteria to assign helix topography. One method chosen was the analysis of the effect of quenchers on Trp λ_{max}. This approach can distinguish intermediate Trp depths arising

from the presence of a mixture of deep and shallow Trp populations from cases in which Trp locates at a relatively uniform intermediate depth (*1*, *24*). A second method was to evaluate the effect of bilayer width upon Trp λ_{max} and depth as assayed by DQA.

When these methods were combined, they were able to distinguish normal TM topography from truncated TM and non-TM topographies. However, there is one remaining ambiguity. Both the truncated/shifted TM and non-TM topographies tend to give red-shifted fluorescence and shallow Trp depth. If they happened to possess a Trp with the same λ_{max} and sensitivity to quenching, then these properties would be insensitive to bilayer width and might be mistaken for a case in which the helix was in the non-TM state at all bilayer widths. The only cases with a relatively bilayer-width-independent λ_{max} were pL(D11), pL(D10D11), and pL(D11D15) at high pH. The non-TM topographies of pL(D11) and pL(D11D15) at high pH are not ambiguous because the deep Trp depth observed in the non-TM state (because of Trp facing the bilayer core) is not consistent with a truncated TM state, which would place the Trp close to the bilayer surface. (If these peptides formed the truncated/shifted TM state their Trp should have had a depth that was very shallow and given Q values higher for pL(D10) at high pH. Instead, they show low Q values.) Furthermore, both Asp residues of pL(D11D15) should be charged at high pH. The longest uninterrupted hydrophobic stretches under these conditions (7 residues) would clearly be too short to form even a truncated TM helix (*1*). The only other case to consider is that of the pL(D10D11) peptide. This peptide is unlikely to form the truncated TM state at high pH because it could only form a truncated hydrophobic helix as long as that of pL(D11), and pL(D11) cannot form a stable truncated TM state.

Ionization Behavior of Membrane-Inserted Asp Residues. The dependence of the charge of ionizable amino acid residues upon their depth in the bilayer is of interest because of its implications for electrostatic interactions in membranes. Generally, the pK_a values observed for Asp residues in hydrophobic helices (5−8.5) were somewhat elevated relative to those for Asp residues in solution (roughly 5). However, providing a detailed explanation of the dependence of Asp pK_a upon Asp position in the peptide sequence is difficult. One reason is that pK_a values are linked to the appropriate conformational equilibria. In other words, the pK_a values are dependent upon the relative stabilities of the charged and uncharged Asp states in both the normal TM topography (which predominates when the Asp is protonated) and whatever topography predominates when the Asp residue is ionized. This in turn is dependent upon the depth of the Asp residue in each topographical state. In the normal TM topography, Asp depth should be linearly dependent on the Asp position, but Asp depth may be a more complicated function of position in the truncated TM and non-TM states. In addition, whether an Asp is in a position in which it can hydrogen bond to Trp [as in pL(D9) and pL(D10)] might affect the Asp pK_a.

It should be noted that for the experiments in this study samples were always prepared at low pH and then adjusted to higher pH if and when desired. The blue-shifted λ_{max}, strong quenching by 10-DN, and deep Trp depths observed at low pH are all indicative of efficient insertion of the Asp-containing peptides into the lipid bilayers. This is also consistent with previous studies, in which it was established that polyLeu peptides efficiently inserted into lipid bilayers even when they contained one or two charged residues in their hydrophobic core (*1*). However, we found during the present study that preparation at low pH was necessary to obtain reproducible λ_{max} values in several cases. Presumably, the charged Asp that might be present if samples were prepared at neutral pH could sometimes interfere with proper insertion of some peptides during vesicle formation.

Relationship of Changes in Helix Topography Because of Asp Residues to Oligomerization. An interesting question is whether any helix topography in the presence of Asp residues is affected by Asp-dependent or Asp-ionization-dependent oligomerization. Several lines of evidence suggest that, when Asp residues are protonated, there is no Asp-dependent oligomerization for the peptides studied in this paper. First, it should be noted that the peptides studied in this paper are flanked by four cationic residues, and previous studies have shown that repulsions between these charges minimize oligomerization of polyLeu sequences and do so even when the total flanking charge is reduced to +2 (*18*). Second, it was shown in two studies that oligomerization is accompanied by a red shift in Trp fluorescence that is not associated with shallow Trp depth (*13*, *18*). This conclusion was confirmed by bromo-Tyr and self-quenching oligomerization assays (*13*, *18*). In the cases in which Trp−Asp interactions were not a factor, the highly blue-shifted Trp fluorescence that we observed in this paper is not consistent with oligomerization. (Of course, this criterion cannot be applied to the peptides in which there is a direct Trp−Asp interaction because they show a red shift.) A third and more widely applicable criterion arises from the previous observation that oligomerization, which would reduce the exposure of Trp to its surrounding environment, is accompanied by reduced accessibility to both lipid-bound and aqueous quenchers (*13*, *18*). There is no reduction in accessibility to quenching for the peptides containing protonated Asp residues relative to that previously observed for analogous peptides without Asp (*13*). (It should be noted that the affect of oligomerization upon quenching does not greatly affect *depth* measurements because they depend on a *Q ratio*, which tends to cancel out the effects of oligomerization.) We also believe that it is unlikely that there is a strong degree of oligomerization in states in which the Asp residue has ionized and shifted to a shallow location in the bilayer. The study of Lear et al. (*12*) shows that even those residues that strongly promote helix oligomerization when located deep within the bilayer (Asn and Gln) lose that ability when they are located at the polar/apolar boundary.

Other Studies of the Effects of Asp Residues Upon the Boundary of the Membrane-Inserted Segment of a Hydrophobic Sequence. Jones and Gierasch previously examined the effect of introducing ionizable residues into hydrophobic LamB signal sequence peptides using Trp fluorescence as a probe, analogous to the strategy used in this paper (*16*). Signal sequence peptides are often not as long or hydrophobic as most TM helices but may show behavior that is analogous to that of TM helices. They interpreted their results in terms of a model in which the main population of peptides inserted into only one leaflet of the bilayer. LamB peptide variants remained at least partially inserted in the presence of

ionizable residues, although not as deep as in their absence. In the case of Asp residues in the hydrophobic core of the peptide, they proposed a structure in which the presumably protonated Asp residue was located near the bilayer surface.

In a series of studies, von Heijne and colleagues have examined the effect of sequence upon the positioning of membrane-inserted helices in endoplasmic reticulum (ER) membranes using a glycosylation-mapping technique (*4*, *8*, *17*, *31*, *32*). This method specifies the position of hydrophobic sequences based on the identification of the residue at the lumenal boundary of the ER membrane. This method may be probing behavior when helices are fully or partly translocon bound, but controls suggest that the behavior observed is similar to that for helices fully inserted in lipid bilayers (*31*).

In a glycosylation-mapping study, Monne et al. showed that the introduction of Asp residues into hydrophobic sequences tended to shift the position of the boundary of the membrane-inserted segment so that the Asp residue was positioned near the bilayer surface (*4*). Because glycosylation mapping is performed near physiological pH, it is very likely that the Asp residues being probed were at least partly ionized, and thus these results are in agreement with the observation in this report that charged Asp tends to locate near the bilayer surface. On the other hand, the absolute Asp-induced shift observed by glycosylation was relatively modest. Introduction of an Asp five residues from the end of a hydrophobic sequence induced a shift in the positioning of the end of the hydrophobic sequence by only about one to two residues. As proposed by Monne et al., this may be because glycosylation mapping may have been measuring the average position for helices equilibrating between a deeper state with a protonated Asp and a shallower state with a charged Asp (*4*).

Examples of Functionally Important Changes in TM α-Helix Positioning in Membranes. Changes in membrane-inserted hydrophobic helices that maintain a TM state but affect helix positioning in the lipid bilayer can be functionally important. Two well-studied examples from bacteria are the Tar and Trg proteins (*33*−*36*). These bacterial chemoreceptors have two TM helices, one of which is postulated to move in a sliding motion in response to ligand binding (*33*, *37*−*40*). Studies on the Tar protein indicate that there may be up to a 2-Å shift in TM helix 2 in response to ligand binding. Similar results have been shown for the Trg protein, and EPR studies show that its TM helices are loosely packed in the membrane, which would allow for vertical displacement of one helix relative to the other when the ligand binds (*41*). Similar TM helix shifts have also been proposed for a bacterial ser chemoreceptor (*42*). Very recent mutagenesis studies show shift-inducing mutations as well as mutations that prevent shifting can control chemoreceptor signaling (*43*).

The Neu receptor tyrosine kinase is an example of a protein with a TM helix that may undergo a functionally important change in membrane positioning that is affected by the ionization state of an acidic residue. A Val to Glu mutation near the edge of the mutant TM segment in Neu results in oncogenicity (*44*, *45*). Through NMR and oriented IR studies, it was shown that the boundary of the TM sequence was dependent on the ionization state of the Glu, such that when the Glu residue was ionized the boundary was different from that in the wild-type sequence (*44*). When the Glu side chain was charged, the TM portion of the helix repositioned to allow the negatively charged Glu to be located at the bilayer surface (*44*). Whether this repositioning involves a change in helix tilt or a shift in the position of the entire helix is not certain.

In the case of integrins, a change in the positioning of the end of a TM segment has been examined using glycosylation mapping by Armulik et al. (*30*). They found that a Lys near the end of a TM sequence is actually buried in the lipid bilayer. It was suggested that this Lys might aid an activating conformational change in which helix tilt is decreased such that the Lys would be repositioned at the membrane surface.

Implications of Asp-Protonation-Induced Helix Shifts and/or Reorientation for Membrane Protein Behavior in Vivo: Endosomal pH May Affect Topography. It is likely that changes in the TM helix topography resulting from changes in Asp protonation exert important effects in vivo. Eukaryotic membrane proteins that cycle between cytoplasmic and endosomal membranes are exposed on their exoplasmic (extracellular or lumen-facing) surface to a pH that probably shifts from about 7.5 when exposed to the extracellular environment to near 5.5 when exposed to the lumen of endosomes (*46*). Our results show that the ionization state of Asp (and presumably Glu) residues within TM segments would generally change from mainly ionized to mainly protonated upon this pH change. For proteins with Asp and Glu residues within their hydrophobic core, alternating exposure to neutral and low pH could induce reversible TM helix shifts and/or conversion between TM and non-TM states. pH effects may even be important for proteins with hydrophobic helices that have acidic residues at or just outside of the putative edge of their hydrophobic core. Protonation/deprotonation of such residues could affect what residue forms the end of the hydrophobic sequence and thus also induce shifts in the TM helix position.

REFERENCES

1. Caputo, G. A., and London, E. (2003) Cumulative effects of amino acid substitutions and hydrophobic mismatch upon the transmembrane stability and conformation of hydrophobic α-helices, *Biochemistry 42*, 3275−3285.
2. Gratkowski, H., Lear, J. D., and DeGrado, W. F. (2001) Polar side chains drive the association of model transmembrane peptides, *Proc. Natl. Acad. Sci. U.S.A. 98*, 880−885.
3. Landolt-Marticorena, C., Williams, K. A., Deber, C. M., and Reithmeier, R. A. (1993) Nonrandom distribution of amino acids in the transmembrane segments of human type I single span membrane proteins, *J. Mol. Biol. 229*, 602−608.
4. Monne, M., Nilsson, I., Johansson, M., Elmhed, N., and von Heijne, G. (1998) Positively and negatively charged residues have different effects on the position in the membrane of a model transmembrane helix, *J. Mol. Biol. 284*, 1177−1183.
5. Ren, J., Lew, S., Wang, Z., and London, E. (1997) Transmembrane orientation of hydrophobic α-helices is regulated both by the relationship of helix length to bilayer thickness and by the cholesterol concentration, *Biochemistry 36*, 10213−10220.
6. Russ, W. P., and Engelman, D. M. (2000) The GxxxG motif: A framework for transmembrane helix−helix association, *J. Mol. Biol. 296*, 911−919.
7. Fleming, K. G., and Engelman, D. M. (2001) Specificity in transmembrane helix−helix interactions can define a hierarchy of stability for sequence variants, *Proc. Natl. Acad. Sci. U.S.A. 98*, 14340−14344.
8. Hermansson, M., and von Heijne, G. (2003) Inter-helical hydrogen bond formation during membrane protein integration into the ER membrane, *J. Mol. Biol. 334*, 803−809.

9. Zhou, F. X., Cocco, M. J., Russ, W. P., Brunger, A. T., and Engelman, D. M. (2000) Interhelical hydrogen bonding drives strong interactions in membrane proteins, *Nat. Struct. Biol. 7*, 154−160.
10. Chin, C. N., and von Heijne, G. (2000) Charge pair interactions in a model transmembrane helix in the ER membrane, *J. Mol. Biol. 303*, 1−5.
11. Zhou, F. X., Merianos, H. J., Brunger, A. T., and Engelman, D. M. (2001) Polar residues drive association of polyleucine transmembrane helices, *Proc. Natl. Acad. Sci. U.S.A. 98*, 2250−2255.
12. Lear, J. D., Gratkowski, H., Adamian, L., Liang, J., and DeGrado, W. F. (2003) Position-dependence of stabilizing polar interactions of asparagine in transmembrane helical bundles, *Biochemistry 42*, 6400−6407.
13. Ren, J., Lew, S., Wang, J., and London, E. (1999) Control of the transmembrane orientation and interhelical interactions within membranes by hydrophobic helix length, *Biochemistry 38*, 5905−5912.
14. Vogt, B., Ducarme, P., Schinzel, S., Brasseur, R., and Bechinger, B. (2000) The topology of lysine-containing amphipathic peptides in bilayers by circular dichroism, solid-state NMR, and molecular modeling, *Biophys. J. 79*, 2644−2656.
15. Harzer, U., and Bechinger, B. (2000) Alignment of lysine-anchored membrane peptides under conditions of hydrophobic mismatch: a CD, ^{15}N, and ^{31}P solid-state NMR spectroscopy investigation, *Biochemistry 39*, 13106−13114.
16. Jones, J. D., and Gierasch, L. M. (1994) Effect of charged residue substitutions on the membrane-interactive properties of signal sequences of the *Escherichia coli* LamB protein, *Biophys. J. 67*, 1534−1545.
17. Monne, M., and von Heijne, G. (2001) Effects of "hydrophobic mismatch" on the location of transmembrane helices in the ER membrane, *FEBS Lett. 496*, 96−100.
18. Lew, S., Caputo, G. A., and London, E. (2003) The effect of interactions involving ionizable residues flanking membrane-inserted hydrophobic helices upon helix−helix interaction, *Biochemistry 42*, 10833−10842.
19. Lew, S., Ren, J., and London, E. (2000) The effects of polar and/or ionizable residues in the core and flanking regions of hydrophobic helices on transmembrane conformation and oligomerization, *Biochemistry 39*, 9632−9640.
20. Killian, J. A., and von Heijne, G. (2000) How proteins adapt to a membrane−water interface, *Trends Biochem. Sci. 25*, 429−434.
21. Segrest, J. P., De Loof, H., Dohlman, J. G., Brouillette, C. G., and Anantharamaiah, G. M. (1990) Amphipathic helix motif: Classes and properties, *Proteins 8*, 103−117.
22. Strandberg, E., and Killian, J. A. (2003) Snorkeling of lysine side chains in transmembrane helices: How easy can it get? *FEBS Lett. 544*, 69−73.
23. Lew, S., and London, E. (1997) Simple procedure for reversed-phase high-performance liquid chromatographic purification of long hydrophobic peptides that form transmembrane helices, *Anal. Biochem. 251*, 113−116.
24. Caputo, G. A., and London, E. (2003) Using a novel dual fluorescence quenching assay for measurement of tryptophan depth within lipid bilayers to determine hydrophobic α-helix locations within membranes, *Biochemistry 42*, 3265−3274.
25. Sreerama, N., Venyaminov, S. Y., and Woody, R. W. (1999) Estimation of the number of α-helical and *β*-strand segments in proteins using circular dichroism spectroscopy, *Protein Sci. 8*, 370−380.
26. Sreerama, N., Venyaminov, S. Y., and Woody, R. W. (2000) Estimation of protein secondary structure from circular dichroism spectra: Inclusion of denatured proteins with native proteins in the analysis, *Anal. Biochem. 287*, 243−251.
27. Provencher, S. W., and Glockner, J. (1981) Estimation of globular protein secondary structure from circular dichroism, *Biochemistry 20*, 33−37.
28. Johnson, W. C. (1999) Analyzing protein circular dichroism spectra for accurate secondary structures, *Proteins 35*, 307−312.
29. Lewis, B. A., and Engelman, D. M. (1983) Lipid bilayer thickness varies linearly with acyl chain length in fluid phosphatidylcholine vesicles, *J. Mol. Biol. 166*, 211−217.
30. Armulik, A., Nilsson, I., von Heijne, G., and Johansson, S. (1999) Determination of the border between the transmembrane and cytoplasmic domains of human integrin subunits, *J. Biol. Chem. 274*, 37030−37034.
31. Nilsson, I., Saaf, A., Whitley, P., Gafvelin, G., Waller, C., and von Heijne, G. (1998) Proline-induced disruption of a transmembrane α-helix in its natural environment, *J. Mol. Biol. 284*, 1165−1175.
32. Nilsson, I., and von Heijne, G. (1998) Breaking the camel's back: Proline-induced turns in a model transmembrane helix, *J. Mol. Biol. 284*, 1185−1189.
33. Chervitz, S. A., and Falke, J. J. (1995) Lock on/off disulfides identify the transmembrane signaling helix of the aspartate receptor, *J. Biol. Chem. 270* (41), 24043−24053.
34. Falke, J. J., and Hazelbauer, G. L. (2001) Transmembrane signaling in bacterial chemoreceptors, *Trends Biochem. Sci. 26*, 257−265.
35. Lee, G. F., Dutton, D. P., and Hazelbauer, G. L. (1995) Identification of functionally important helical faces in transmembrane segments by scanning mutagenesis, *Proc. Natl. Acad. Sci. U.S.A. 92*, 5416−5420.
36. Lee, G. F., and Hazelbauer, G. L. (1995) Quantitative approaches to utilizing mutational analysis and disulfide cross-linking for modeling a transmembrane domain, *Protein Sci. 4*, 1100−1107.
37. Beel, B. D., and Hazelbauer, G. L. (2001) Signaling substitutions in the periplasmic domain of chemoreceptor Trg induce or reduce helical sliding in the transmembrane domain, *Mol. Microbiol. 40*, 824−834.
38. Chervitz, S. A., Lin, C. M., and Falke, J. J. (1995) Transmembrane signaling by the aspartate receptor: Engineered disulfides reveal static regions of the subunit interface, *Biochemistry 34*, 9722−9733.
39. Baumgartner, J. W., and Hazelbauer, G. L. (1996) Mutational analysis of a transmembrane segment in a bacterial chemoreceptor, *J. Bacteriol. 178*, 4651−4660.
40. Hughson, A. G., and Hazelbauer, G. L. (1996) Detecting the conformational change of transmembrane signaling in a bacterial chemoreceptor by measuring effects on disulfide cross-linking in vivo, *Proc. Natl. Acad. Sci. U.S.A. 93*, 11546−11551.
41. Barnakov, A., Altenbach, C., Barnakova, L., Hubbell, W. L., and Hazelbauer, G. L. (2002) Site-directed spin labeling of a bacterial chemoreceptor reveals a dynamic, loosely packed transmembrane domain, *Protein Sci. 11*, 1472−1481.
42. Isaac, B., Gallagher, G. J., Balazs, Y. S., and Thompson, L. K. (2002) Site-directed rotational resonance solid-state NMR distance measurements probe structure and mechanism in the transmembrane domain of the serine bacterial chemoreceptor, *Biochemistry 41*, 3025−3036.
43. Miller, A. S., and Falke, J. J. (2004) Side chains at the membrane−water interface modulate signaling state of a transmembrane receptor, *Biochemistry 44*, 1763−1770.
44. Smith, S. O., Smith, C. S., and Bormann, B. J. (1996) Strong hydrogen bonding interactions involving a buried glutamic acid in the transmembrane sequence of the neu/erbB-2 receptor, *Nat. Struct. Biol. 3*, 252−258.
45. Surti, T., Klein, O., Aschheim, K., DiMaio, D., and Smith, S. O. (1998) Structural models of the bovine papillomavirus E5 protein, *Proteins 33*, 601−612.
46. Sandvig, K., and Olsnes, S. (1980) Diphtheria toxin entry into cells is facilitated by low pH, *J. Cell. Biol. 87*, 828−832.
47. Chung, L. A., Lear, J. D., and DeGrado, W. F. (1992) Fluorescence studies of the secondary structure and orientation of a model ion channel peptide in phospholipid vesicles, *Biochemistry 31*, 6608−6616.

BI049696P